[7] H. Komizo *et al.*, "Improvement of nonlinear distortion in an IMPATT stable amplifier," *IEEE Trans. Microwave Theory Tech.*, vol. MTT-21, pp. 721–728, Nov. 1973.
[8] G. L. Heiter, "Characterization of nonlinearities in microwave devices and systems," *IEEE Trans. Microwave Theory Tech.*, vol. MTT-21, pp. 797–805, Dec. 1973.
[9] H. J. Kuno, "Analysis of nonlinear characteristics and transient response of IMPATT amplifiers," *IEEE Trans. Microwave Theory Tech.*, vol. MTT-21, Nov. 1973.
[10] M. E. Hines, "Negative-resistance diode power amplification," *IEEE Trans. Electron. Devices*, vol. ED-17, pp. 1–8, Jan. 1970.
[11] H. Van Trees, *Synthesis of Optimum Nonlinear Control Systems.* Cambridge, MA: M.I.T. Press, 1962.
[12] E. Bedrosian and S. O. Rice, "The output properties of Volterra systems (nonlinear systems with memory) driven by harmonic and Gaussian inputs," *Proc. IEEE*, vol. 59, pp. 1688–1707, Dec. 1971.
[13] P. Bura *et al.*, "Highly linear medium power, 11 GHz FET amplifier," *ISSCC Digest of Technical Papers*, pp. 158–159, Feb. 1976.

Effects of Depletion-Layer Modulation on Spurious Oscillations in IMPATT Diodes

D. TANG, MEMBER, IEEE, AND G. I. HADDAD, FELLOW, IEEE

Abstract—**A theoretical analysis of the effects of depletion-layer modulation on spurious oscillations in IMPATT diodes is given. The relationship between the magnitude of the depletion-layer modulation, circuit impedance and threshold for degenerate instabilities is presented.**

I. Introduction

IMPATT diode microwave amplifiers and oscillators frequently exhibit certain spurious "parametric oscillations" near or at the subharmonic of the signal frequency, when the RF excitation exceeds a threshold level, which is dependent upon the device and circuit and often occurs below the power saturation point. Hines [1], Peterson [2], and Schroeder [3] gave detailed analyses on these parametric effects for a Read-type diode. They analyzed the parametric instabilities based on the nonlinear relationship between the avalanche current and the voltage across the avalanche region. Parametric components (at frequencies other than the pump frequency but whose sum is equal to the pump frequency) may exist in these devices. These current components flow through the drift region, experience a phase change and induce a current in the external circuit. The interaction between the current components and the circuit may lead to self-sustaining voltages at these parametrically related frequencies even without any external sources at these frequencies. The expressions for determining the instability threshold were given in [1, eqs. (23) and (35)]. It was emphasized there that circuit impedance may either suppress or enhance the occurrence of the instability. Based on the work of Hines [1], Schroeder [3] derived the circuit impedance conditions required for unconditional stable operation and for avoiding parametric instabilities in the IMPATT diode circuit.

Generally, the IMPATT diode has a nonpunch-through structure and its depletion-layer width is modulated considerably by the RF voltage [4], [5]. The objective of the present investigation is to examine the effect of the depletion-layer-width modulation on the parametric instabilities. The original analysis of [1] concerning the parametric components in the avalanche region is retained [1, (1)–(16)]. The change of the phase relationship in the drift region is examined including the nonlinear capacitance effect, and due to the complexity of the mathematics some assumptions are made. These assumptions and results are discussed as they arise.

II. Theoretical Analysis

A typical high-efficiency structure for an IMPATT diode is selected for this analysis. It is of the low–high–medium doping type. Fig. 1 shows the electric field profile of this structure. The metallurgical junction is at $x = 0$. The diode is divided conceptually into an avalanche region with fixed width x_a and a drift region with a time-varying width x_d, which is approximately proportional to the square root of the terminal instantaneous voltage. The RF terminal voltage consists of two parts. One is the large microwave periodic excitation, called the pump signal, at frequency ω_p, and the other is a small applied signal at frequency ω_0, which may or may not be harmonically related to the pump frequency. This small signal is applied as a perturbation and is assumed to be sinusoidal. Because of the nonlinearity of the avalanche process, multiple responses occur at various new frequencies that are sums and differences of the various harmonics of the frequencies applied. The main interest here

Manuscript received September 15, 1975; revised November 15, 1976. This work was supported by the Air Force Systems Command, Rome Air Development Center, under Contract F30602-74-C-0012. It was also partially sponsored by the Air Force Office of Scientific Research, Air Force Systems Command, USAF, under Grant AFOSR-76-2939.

D. Tang is with IBM, Thomas J. Watson Research Center, Yorktown Heights, NY 10598.
G. I. Haddad is with the Department of Electrical and Computer Engineering, University of Michigan, Ann Arbor, MI 48109.

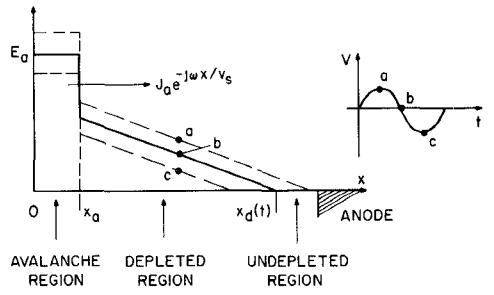

Fig. 1. Field profile of a low-high-medium doped IMPATT diode.

will be in the applied signal below the pump frequency and its image frequency $\omega_{-1} = \omega_p - \omega_0$. It has been shown that the avalanche region behaves as a nonlinear inductor in parallel with a linear capacitor, and the current–voltage relationship is given as [1]

$$\begin{bmatrix} I_{a0} \\ I^*_{a-1} \end{bmatrix} = [Y_a] \begin{bmatrix} V_{a0} \\ V^*_{a-1} \end{bmatrix} \tag{1}$$

where the subscripts 0 and -1 indicate quantities at frequency ω_0 and ω_{-1}, respectively. V_a and I_a are the avalanche-region voltage and particle current, respectively, and both are sinusoidal (the time-dependent terms $e^{j\omega_0 t}$ and $e^{-j\omega_{-1}t}$ are suppressed). $[Y_a]$ is a 2×2 matrix and is given by

$$[Y_a] = \begin{bmatrix} \dfrac{1}{j\omega_0 L_a} & \dfrac{-M_1}{j\omega_{-1} L_a} \\ \dfrac{M_{-1}}{j\omega_0 L_a} & -\dfrac{1}{j\omega_{-1} L_a} \end{bmatrix} \tag{2}$$

where

$L_a = \tau_a / 2 I_0 \alpha'$

τ_a = the avalanche region transit time

I_0 = the dc current

$\alpha' = d\alpha/dE$

α = the field dependent ionization rate

$M_{\pm 1} = I_{\pm 1}/I_0$

$I_{\pm 1}$ = the fundamental Fourier components of the pump current.

The total current $[I_t]$ is the sum of the avalanche (particle) current and the displacement current $j\omega C_a$

$$\begin{bmatrix} I_{t0} \\ I^*_{t-1} \end{bmatrix} = \begin{bmatrix} j\omega_0 C_a(1-\xi_0) & -\dfrac{M_1}{j\omega_{-1} L_a} \\ \dfrac{M_1}{j\omega_0 L_a} & -j\omega_{-1} C_a(1-\xi_{-1}) \end{bmatrix} \cdot \begin{bmatrix} V_{a0} \\ V^*_{a-1} \end{bmatrix} \tag{3}$$

or

$$[I_t] \triangleq [Y_{at}][V_a]$$

where

$C_a = \varepsilon A / x_a$

$\xi_0 = (\omega_a/\omega_0)^2 = 1/L_a C_a \omega_0^2$

$\xi_{-1} = (\omega_a/\omega_{-1})^2 = 1/L_a C_a \omega_{-1}^2$

A = the cross-sectional area.

It is assumed that the avalanche current generated in the avalanche region drifts "undistorted" through the drift region at the saturated drift velocity v_s. The short section near the end of the drift region, where the carrier velocity is not saturated, is neglected.

Therefore the avalanche current in the drift region is equal to $J_a e^{-j\omega x/v_s}$. The local electric field $E(x)$ induced by this particle current is given by

$$\varepsilon \frac{dE(x)}{dt} = J_t - J_a e^{-j\omega x/v_s}$$

or

$$A \cdot \varepsilon \begin{bmatrix} j\omega_0 E_0 \\ -j\omega_{-1} E^*_{-1} \end{bmatrix} = \begin{bmatrix} I_{t0} \\ I^*_{t-1} \end{bmatrix} - \begin{bmatrix} I_{a0} e^{-j\omega_0 x/v_s} \\ I^*_{a-1} e^{j\omega_{-1} x/v_s} \end{bmatrix}. \tag{4}$$

Therefore the drift region voltage can be found by integrating the electric field E over the drift region, i.e., $V_d = \int_0^{x_d(t)} E\, dx$ or

$$A \cdot \varepsilon \begin{bmatrix} j\omega_0 V_0 \\ -j\omega_{-1} V^*_{-1} \end{bmatrix} = x_d \begin{bmatrix} I_{t0} \\ I^*_{t-1} \end{bmatrix} - \begin{bmatrix} x_d \bar{k}_0 I_{a0} \\ x_d \bar{k}^*_{-1} I^*_{a-1} \end{bmatrix} \tag{5}$$

where V_d is the voltage across the drift region, $\bar{k}_m = [1 - \exp(-j\bar{\theta}_m)]/j\bar{\theta}_m$, $\bar{\theta}_m = \omega_m x_d / v_s$ and $m = 0, -1$. This equation can be reduced to [1, (18)] if x_d is constant (so is $\bar{k}_m$) and x_d is defined as $\varepsilon A/\bar{C}_d$, where $\bar{C}_d$ is the capacitance of the drift region.

Since the drift region width varies as a function of time at the pump frequency, it is assumed that

$$x_d = x_0 + x_1 e^{j\omega_p t} + x_{-1} e^{-j\omega_p t} + \cdots \tag{6}$$

and the x_1, x_{-1} are either real or complex quantities depending on the time origin chosen. From a Taylor series expansion of $x_d \bar{k}_m$ and neglecting higher order products such as $x_1 x_{-1}$ we obtain

$$\begin{aligned} x_d \bar{k}_m &= x_d \bar{k}_m \Big|_{x_d = x_0} + (x_d - x_0) \frac{d(x_d \bar{k}_m)}{dx_d}\Big|_{x_d = x_0} + \cdots \\ &= \frac{x_0(1 - e^{-j\omega_m x_0/v_s})}{j\dfrac{\omega_m x_0}{v_s}} \\ &\quad + (x_1 e^{j\omega_p t} + x_{-1} e^{-j\omega_p t})(e^{-j\omega_m x_0/v_s}). \end{aligned}$$

Therefore (5) becomes

$$\begin{aligned} A \cdot \varepsilon \begin{bmatrix} j\omega_0 V_{d0} \\ -j\omega_{-1} V^*_{d-1} \end{bmatrix} &= \begin{bmatrix} x_0 & x_1 \\ x_{-1} & x_0 \end{bmatrix} \begin{bmatrix} I_{t0} \\ I^*_{t-1} \end{bmatrix} \\ &\quad - \begin{bmatrix} x_0 k_0 & x_1 e^{-j\theta_0} \\ x_{-1} e^{+j\theta_{-1}} & x_0 k^*_{-1} \end{bmatrix} \begin{bmatrix} I_{a0} \\ I^*_{a-1} \end{bmatrix} \end{aligned} \tag{7}$$

where

$k_0 = \bar{k}_0|_{x_d = x_0}$

$k_{-1} = \bar{k}_{-1}|_{x_d = x_0}$

$\theta_0 = x_0 \omega_0 / v_s$

and

$\theta_{-1} = x_0 \omega_{-1} / v_s$.

Dividing both sides of (7) by $j\omega\varepsilon A$ and defining

$$C_d = \varepsilon A/x_0$$

and

$$C_{\pm 1} = \varepsilon A/x_{\pm 1}$$

yields

$$\begin{bmatrix} V_{d0} \\ V^*_{d-1} \end{bmatrix} = [x] \begin{bmatrix} I_{t0} \\ I^*_{t-1} \end{bmatrix} - [xk] \begin{bmatrix} I_{a0} \\ I^*_{a-1} \end{bmatrix} \tag{8}$$

where

$$[x] = \begin{bmatrix} \dfrac{1}{j\omega_0 C_d} & \dfrac{1}{j\omega_0 C_1} \\ \dfrac{1}{-j\omega_{-1} C_{-1}} & \dfrac{1}{-j\omega_{-1} C_d} \end{bmatrix}$$

and

$$[xk] = \begin{bmatrix} \dfrac{k_0}{j\omega_0 C_d} & \dfrac{e^{-j\theta_0}}{j\omega_0 C_1} \\ \dfrac{e^{j\theta_{-1}}}{-j\omega_{-1} C_{-1}} & \dfrac{-k^*_{-1}}{j\omega_{-1} C_d} \end{bmatrix}.$$

The terminal voltage of the diode is the sum of $[V_a]$ and $[V_d]$, and from (1) and (2) the total voltage across the diode $[V_t]$ is given as

$$\begin{aligned}[V_t] &= [V_a] + [V_d] = [V_a] + [x][I_t] - [xk][I_a] \\ &= \{[U] + [x][Y_{at}] - [xk][Y_a]\}[V_a] \end{aligned} \tag{9}$$

where $[U]$ is the unitary matrix

$$\begin{bmatrix} 1 & 0 \\ 0 & 1 \end{bmatrix}.$$

The Kirchhoff voltage equation for the diode and the circuit is (see Fig. 2)

$$[V_x] = [Z_x][I_t] + [V_t] \tag{10}$$

where $[Z_x]$ = the external circuit impedance matrix:

$$[Z_x] = \begin{bmatrix} Z_{x,0} & 0 \\ 0 & Z^*_{x,-1} \end{bmatrix}$$

$Z_{x,m} = Z_x(\omega_m)$ and $[V_x]$ is the external voltage source. Equation (10) can be written in terms of $[V_a]$ by substituting (9) and (3) into it. This yields

$$\begin{aligned}[V_x] &= [Z_x][Y_{at}][V_a] + \{[U] + [x][Y_{at}] - [xk][Y_a]\}[V_a] \\ &= \{[U] + ([Z_x] + [x])[Y_{at}] - [xk][Y_a]\}[V_a] \\ &\triangleq [P][V_a] \end{aligned} \tag{11}$$

where

$$[P] = \begin{bmatrix} \xi_0 C_a(A_0 - B_0 C_1^{-1} M_{-1}), & \dfrac{\omega_a^2}{\omega_0 \omega_{-1}} C_a(-C_1^{-1} F_{0,-1} + D_0 M_1) \\ \dfrac{\omega_a^2 C_a}{\omega_0 \omega_{-1}}(-F^*_{-1,0} C_{-1}^{-1} + D^*_{-1} M_{-1}), & \xi_{-1} C_a(A^*_{-1} - B^*_{-1} C_{-1}^{-1} M_1) \end{bmatrix}$$

$$A_m = j\omega_m \left(\frac{1-\xi_m}{\xi_m}\right)(Z_{x,m} + Z_{d,m})$$

$$B_m = 1 - e^{-j\theta_m},\ C_{\pm 1}^{-1} = 1/C_{\pm 1}$$

$$D_m = j\omega_m \left(Z_{x,m} + \frac{1-k_m}{j\omega_m C_d}\right)$$

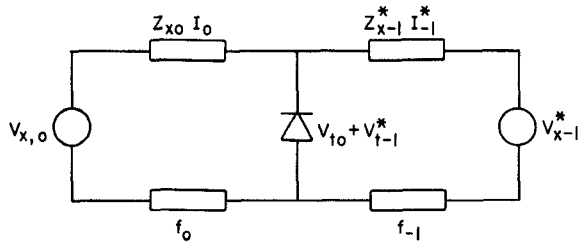

Fig. 2. Equivalent circuit for parametric interaction in an IMPATT diode circuit (f_m = ideal bandpass filter at ω_m, $m = 0, -1$).

$$F_{m,n} = \frac{1}{\xi_n} - B_m$$

$$m = 0, -1$$

$$Z_{d,m} = Z_d(\omega_m)$$

= the small-signal diode impedance at ω_m

$$= \frac{1}{j\omega_m C_a}\left[\frac{1}{1-\xi_m}\right] + \frac{1}{j\omega_m C_d}\left(1 - \frac{\xi_m k_m}{\xi_m - 1}\right)$$

and

$$\xi_m = \left(\frac{\omega_a}{\omega_m}\right)^2.$$

There is an infinite set of nonzero solutions to $[V_a]$ when both $[V_x]$ and the determinant of $[P]$ are zero. Under such a condition the diode-circuit system is unstable and the signal and its image can be self-excited parametrically without any external source. Therefore the condition

$$\det [P] = 0 \tag{12}$$

determines the stability criterion. If $\det [P] \neq 0$, the system is stable. From (12) the following is obtained:

$$\begin{aligned}&(A_0 - B_0 C_1^{-1} M_{-1})(A^*_{-1} - B^*_{-1} C_{-1}^{-1} M_1) \\ &- (-C_1^{-1} F_{0,-1} + D_0 M_1) \\ &\qquad \cdot (-F^*_{-1,0} C_{-1}^{-1} + D^*_{-1} M_{-1}) = 0. \end{aligned} \tag{13}$$

Furthermore, neglecting terms containing a $C_1^{-1} C_{-1}^{-1}$ product yields

$$\begin{aligned}&(A_0 A^*_{-1} - D_0 D^*_{-1} M_1 M_{-1}) \\ &- M_1[A_0 B^*_{-1} C_{-1}^{-1} - D_0 F^*_{-1,0} C_{-1}^{-1}] \\ &\qquad - M_{-1}[A^*_{-1} B_0 C_1^{-1} - D^*_{-1} F_{0,-1} C_1^{-1}] = 0. \end{aligned} \tag{14}$$

A simple equation can be obtained if the degenerate case is considered ($\omega_0 = \omega_{-1} = \omega_p/2$). This is

$$\begin{aligned}&|A_0|^2(1 - |S_0|^2 M_1^2) - 2 \cdot \mathrm{Re} \cdot [C_{-1}^{-1} M_1(A_0 B_0^* - D_0 F_{0,0}^*)] \\ &= 0 \end{aligned} \tag{15}$$

where

$$S_m = \frac{-D_m}{A_m} = 1 + \frac{1}{\xi_m - 1} \frac{Z_{x,m} + \dfrac{1}{j\omega_m C_T}}{Z_{x,m} + Z_{d,m}}.$$

Re ( ) is the real part of the quantity. Note that (15) becomes identical with [1, (35)] if the depletion-region modulation is zero or $C_{-1}^{-1} = 0$.

It is clear that the left-hand side of (15) is always greater than zero as M_1 approaches zero. As M_1 increases, there exists a value M_{1T} at which (15) is satisfied. This particular value M_{1T} is the threshold pump level for subharmonic instabilities. In other words, when the pump level reaches this threshold, the diode-circuit system is unstable and spurious oscillation at the subharmonic frequency occurs. For a given diode, the threshold pump level is dependent upon the circuit impedance at the subharmonic frequency. There may exist a circuit impedance zone in which the solution of M_1 from (15) is greater than one. However, the value of M_1 cannot be greater than 1 $[M_1 = (I_1/I_{dc})]$. Therefore, the diode is free from subharmonic instabilities when it is operated in this circuit impedance zone. Based on (14), similar arguments can be applied to the nondegenerate-type instabilities [1], i.e., the instabilities occur at two frequencies with their sum being equal to the pump frequency. In such a case, the circuit impedance at each instability frequency must be included in the consideration. However, due to the complexity of the analysis, only the degenerate case is considered here.

Whether the depletion-layer-width modulation enhances or suppresses the subharmonic oscillation in a given circuit is determined by the sign of the second term of (15). When Re ( ) is positive, the left-hand side of (15) reduces to zero at a lower value of M_1, thus the depletion-layer-width modulation enhances instabilities. Otherwise, the opposite will be the case.

To determine the sign of the second term of (15), the phase relation between x_1 and M_1 should be considered. At low pump levels, M_1 is approximately 90 degrees behind the voltage in the avalanche region and it can be assumed that the avalanche voltage is in phase with the pump voltage across the diode. The angle of x_1 can be assumed to be in phase with the pump voltage. At high pump levels where the rectification becomes pronounced, the phase between x_1 and M_1 becomes less than 90 degrees. (The particular value of this phase angle depends on the particular device and the operating point.) One can select a time origin such that $M_1 = M_{-1}$ = real positive, then $x_1 = x^*_{-1} = \bar{x}_1 e^{j\phi}$, where $\bar{x}_1$ = real positive and $0 < \phi < 90$ degrees. Similarly, $C_1 = C^*_{-1} = \bar{C}_1 e^{-j\phi}$ and $\bar{C}_1$ = real positive. Furthermore, by writing $Z_x = R_x + jX_x$ and substituting A_0, B_0, D_0, and $F_{0,0}$ in the diode parameters, the second term of (15) can be rewritten as (see Appendix A)

$$-\frac{2\omega_0 M_1}{\bar{C}_1 \xi_0} \cdot [R_x \sin(\theta_0 - \phi) + X_x \cos(\theta_0 - \phi) + f] \tag{16}$$

where

$$f = \frac{\cos\phi - \cos(\theta_0 - \phi)}{\omega_0 C_T} + \frac{1}{\omega_0 C_d}\left[-\cos\phi - \left(\frac{1-\cos\theta_0}{\theta_0}\right)\cdot \sin\phi + \frac{\sin\theta_0 \cos\phi}{\theta_0}\right].$$

If the value of (16) is negative, the depletion-layer-width modulation effectively raises the threshold M_{1T} of the subharmonic instabilities. Since (16) is a linear function of R_x and X_x, (16) is a straight line in the complex impedance plane. There is an area in the complex impedance plane such that (16) is less than zero. Furthermore, the coefficients of $1/\omega_0 C_T$ and $1/\omega_0 C_d$ are both negative and the coefficient of X_x is positive if $0 < \theta_0 \lesssim 90$ degrees, $0 < \phi < 90$ degrees. The coefficient of R_x may be either positive or negative. Equation (16) is plotted in Fig. 3(a). The solid and dashed lines are for positive and negative coefficients of R_x, respectively. The arrow indicates the area in which (16) is less than zero. Thus there exists a realizable circuit impedance area in which the depletion-layer-width modulation may raise the threshold pump level of the subharmonic instabilities.

Next the effect of the depletion-layer-width modulation on the circuit impedance zone is examined, in which the diode-circuit system is unconditionally stable. In other words, circuit zones that satisfy (15) when $M_1 = M_{1T} = 1$ are of interest. To do this (15) should be examined again. The first term of (15) is a quadratic function of R_x and X_x. It can be shown (see Appendix B) that when this term is written explicitly it is found to be a circle with radius r and center at (R_c, X_c). Since the second term of (15) is a linear function of R_x and X_x, (15) is again a circle but with a different radius and center. Equation (15) can be rewritten as

$$\begin{aligned}
&\omega_0^2\left[\left(\frac{1-\xi_0}{\xi_0}\right)^2 - 1\right]\cdot[(R_x - R_c)^2 + (X_x - X_c)^2 - r^2] \\
&\qquad - \frac{2\omega_0}{\bar{C}_1 \xi}\cdot[\sin(\theta_0 - \phi)R_x + \cos(\theta_0 - \phi)X_x + f] \\
&\triangleq \omega_0^2\left[\left(\frac{1-\xi_0}{\xi_0}\right)^2 - 1\right] \\
&\quad \cdot[(R_x - R_c')^2 + (X_x - X_c')^2 - r'^2] \\
&= 0
\end{aligned} \tag{17}$$

where (R_c', X_c') is the center and r' is the radius of the new circle

$$R_c' = R_c + \frac{1}{g}\frac{\omega_0 \sin(\theta_0 - \phi)}{\bar{C}_1 \xi_0}$$

$$X_c' = X_c + \frac{1}{g}\frac{\omega_0 \cos(\theta_0 - \phi)}{\bar{C}_1 \xi_0}$$

$$g = \omega_0^2\left[\left(\frac{1-\xi_0}{\xi_0}\right)^2 - 1\right]$$

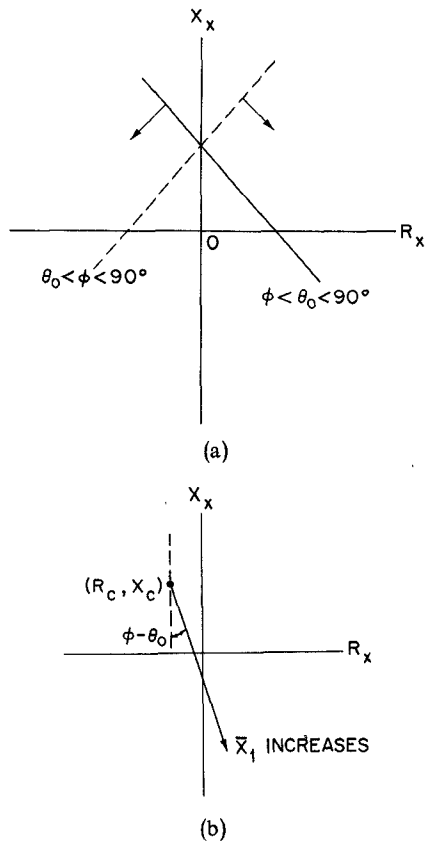

Fig. 3. (a) Circuit zones (indicated by arrows) in which depletion-layer modulation raises the threshold pump level. (b) Locus of the center of the circle (R_c', X_c') of the stable circuit zone.

and

$$r'^2 = r^2 + \frac{2\omega_0 f}{g\bar{C}_1\xi_0} + (R_c'^2 - R_c^2) + (X_c'^2 - X_c^2). \quad (18)$$

Note that, at the subharmonic frequency, usually

$$\xi_0 = \left(\frac{\omega_a}{\omega_0}\right)^2 > 1$$

and

$$g = \omega_0^2\left[\left(\frac{1-\xi_0}{\xi_0}\right)^2 - 1\right] = \omega_0^2\left(\frac{1-2\xi_0}{\xi_0^2}\right) < 0.$$

Therefore, R_c' is greater than R_c if the angle $\theta_0 - \phi$ is negative. The center therefore shifts toward the positive side of the impedance plane. The shift increases as $\bar{x}_1$ increases. Fig. 3(b) shows the locus of the center of the circle for stable operation. When $\bar{x}_1$ is zero, the center of the circle coincides with the center of the circle of a punch-through Read-type diode (R_c, X_c). Thus the stable circuit zone changes as the depletion-layer modulation increases.

III. Examples

The change in the stable circuit zone is calculated for a particular diode structure. The diode is characterized by the following parameters:

$$\omega_a = 2\pi \times 7.5 \times 10^9 \text{ rad/s}$$

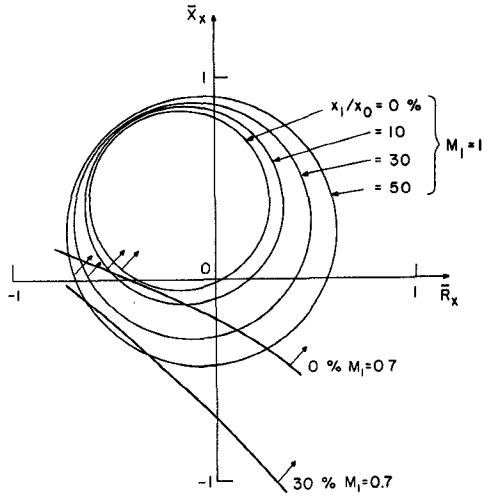

Fig. 4. Normalized circuit impedance for stable operation. Arrows indicate the stable regions. The circuit impedance is normalized to 50 Ω ($\phi = 90$ degrees, $f_0 = f_p/2 = 4$ GHz).

$$\tau_0 = x_0/v_s = 40 \text{ ps}$$

$$C_T = 1 \text{ pF}$$

$$\bar{x}_d = x_0/(x_a + x_d) = x_0/(x_a + x_0) = 0.83$$

where x_0 is the mean drift region width. This set of parameters was used in [3] and is used here for comparison. This diode is typically operated at an X-band frequency. It is assumed that the diode is pumped at 8 GHz and the stable circuit zone is calculated for $\phi = 90$ degrees and $\phi = 60$ degrees. The circuit impedances calculated from (15) as functions of M_1 and $\bar{x}_1/x_0$ are plotted in Fig. 4. In this calculation the angle ϕ is assumed to be 90 degrees. The arrows indicate the impedance zone in which the pump level M_1 is higher than the indicated value. Therefore, these zones are stable zones for the given pump level. As the value of M_1 increases the area of the stable zone shrinks. The circuit zone inside $M_1 = 1$ provides unconditional stable operation.

In this figure it is clear that the stable operation covers a wider area in the right-half plane as the depletion-layer-width modulation increases for both cases of $M_1 = 1.0$ and $M_1 = 0.7$. Since the right-half plane of the circuit is physically realizable, the circuit design condition is therefore loosened when depletion-layer modulation is present.

Fig. 5 gives the circuit-impedance zone for unconditional stable operation at various subharmonic frequencies. The same diode parameters are used in this computation. It is found that the broadening of the stable zone holds over a wide frequency range. Furthermore, a circuit impedance outside the stable region was selected to find the stability threshold. It is $\bar{Z}_x = 0.6 - j.8$ (see Fig. 4). Substituting this $\bar{Z}_x$ into (15) and computing M_1 for various values of $\bar{x}_1/x_0$ gives the results shown in Fig. 6. It is clear that the threshold level M_1 increases as depletion-layer-width modulation increases. For this case it should be noted that this particular circuit impedance satisfies the condition (16) < 0.

Calculations were also made for the case of $M_1 = 1$, $\phi = 60$ degrees, and various values of $\bar{x}_1/x_0$. The results are

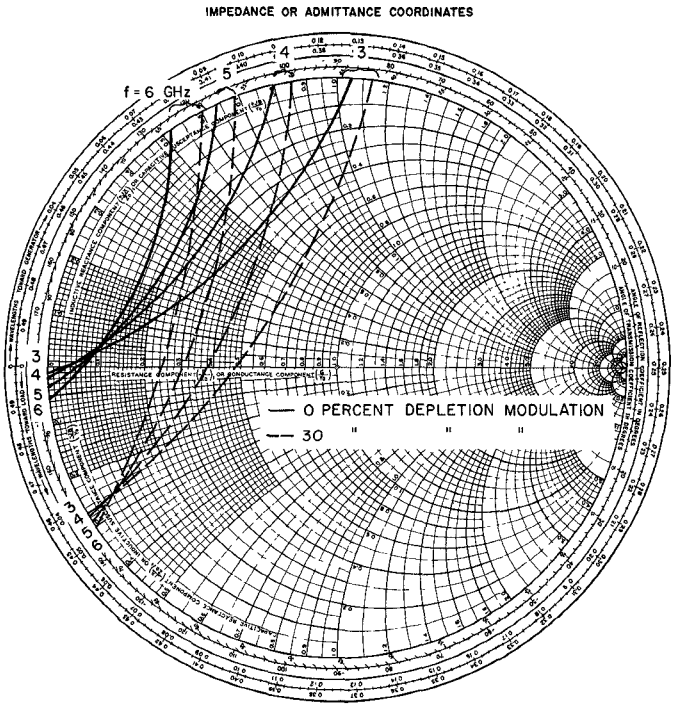

Fig. 5. Stable circuit zone at various subharmonic frequencies. $\bar{x}_1/x_0 = 30$ and 0 percent ($\phi = 90$ degrees, $M_{1T} = 1$).

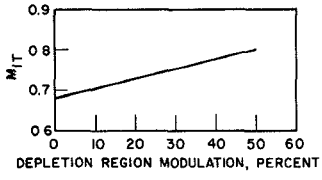

Fig. 6. Threshold M_{1T} versus $\bar{x}_1/x_0$ for a given circuit $Z_x = 30 - j40\ \Omega$ ($f_0 = f_p/2 = 4$ GHz, $\phi = 90$ degrees).

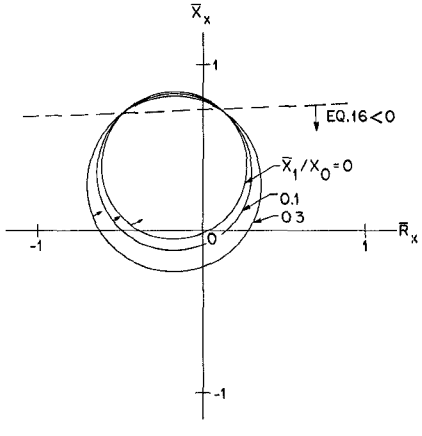

Fig. 7. Normalized circuit impedance for stable operation. Arrow indicates stable region. (Circuit is normalized to 50 Ω, $\phi = 60$ degrees, $f_0 = f_p/2 = 4$ GHz, $M_{1T} = 1$.)

shown in Fig. 7. The stable circuit zone shifts as $\bar{x}_1/x_0$ increases. The region where (16) < 0 is also shown. It is clear that a circuit provides stable operation for the diode with large depletion-layer-width modulation only in the region where (16) < 0. It is also seen from Fig. 7 that the circuit impedance region for stable operation becomes larger as the depletion-layer modulation increases.

IV. Summary

The theoretical analyses of parametric instabilities in the Read-type IMPATT diode were extended to nonpunch-through IMPATT diodes in which the depletion-layer width is modulated by the terminal voltage. Nonlinear frequency mixing takes place in both the avalanche region and the drift region. A two-frequency model was developed in this analysis. In order to obtain a mathematically manageable expression, the unsaturated drift velocity of the carriers at the end of the drift region was not included. This unsaturated velocity introduces another modulation in the carrier transit angle and its effect is beyond the scope of this analysis. Equation (13) describes the threshold pump level at which the parametric instabilities occur. The effect of depletion-layer-width modulation may either raise or lower the value of the threshold pump level of the instabilities depending on the circuit and the phase angle between the depletion-layer-width modulation x_1 and the avalanche current M_1. This relation is given in (16) and is plotted in Fig. 3(a). The circuit zone for stable operation was also examined. The change in the stable circuit zone is summarized in (18). Numerical calculations were made for a particular X-band diode. Generally, when ϕ is close or equal to 90 degrees, the stable circuit zone increases as $\bar{x}_1/x_0$ increases. When the angle ϕ decreases the stable circuit zone moves. The circuit that provides stable operation for the Read-type diode may or may not provide stable operation as the depletion-layer-width modulation increases. This is illustrated in Fig. 7.

Appendix A

The second term of (15) is written explicitly with the circuit and diode parameters:

$$Z_x = R_x + jX_x.$$

Henceforth the subscript 0 is omitted for convenience

$$A = j\omega\left(\frac{1-\xi}{\xi}\right)Z_x + j\omega\left(\frac{1-\xi}{\xi}\right)\left[\frac{1}{j\omega C_a}\left(\frac{1}{1-\xi}\right) + \frac{1}{j\omega C_d}\left(1 - \frac{\xi k}{\xi - 1}\right)\right].$$

Separating A into real and imaginary parts yields

$$A = \left\{-\left(\frac{1-\xi}{\xi}\right)\omega X_x + \frac{1}{\xi}\left[\frac{1}{C_a} - \frac{1}{C_d}\left(\xi - 1 - \xi\frac{\sin\theta}{\theta}\right)\right]\right\} + j\left[\left(\frac{1-\xi}{\xi}\right)\omega R_x - \frac{1-\cos\theta}{\theta}\right]. \quad \text{(A.1)}$$

Similarly,

$$B^* = 1 - \cos\theta - j\sin\theta \tag{A.2}$$

$$\begin{aligned} D &= j\omega\left(Z_x + \frac{1-k}{j\omega C_d}\right) \\ &= \left[-\omega X_x + \frac{1}{C_d}\left(1 - \frac{\sin\theta}{\theta}\right)\right] \\ &\quad + j\left(\omega R_x + \frac{1}{C_d}\frac{1-\cos\theta}{\theta}\right) \end{aligned} \tag{A.3}$$

and

$$\begin{aligned} F^* &= \frac{1}{\xi} - (1 - e^{j\theta}) \\ &= \left(\frac{1}{\xi} - 1 + \cos\theta\right) + j\sin\theta. \end{aligned} \tag{A.4}$$

The products of $A \cdot B^*$ and $D \cdot F^*$ are given by

$$\begin{aligned} \text{Re}\,[AB^*] &= \left\{-\left(\frac{1-\xi}{\xi}\right)\omega X_x \right. \\ &\quad \left. + \frac{1}{\xi}\left[\frac{1}{C_a} - \frac{1}{C_d}\left(\xi - 1 - \xi\frac{\sin\theta}{\theta}\right)\right]\right\} \\ &\quad \cdot (1 - \cos\theta) \\ &\quad + \left[\left(\frac{1-\xi}{\xi}\right)\omega R_x - \left(\frac{1-\cos\theta}{\theta C_d}\right)\right]\sin\theta \\ &= \omega\left(\frac{1-\xi}{\xi}\right)[R_x\sin\theta - X_x(1-\cos\theta)] \\ &\quad + \frac{1}{\xi C_a}(1-\cos\theta) + \frac{1-\cos\theta}{C_d}\left(\frac{1}{\xi} - 1\right) \end{aligned} \tag{A.5}$$

$$\begin{aligned} \text{Im}\,[AB^*] &= \left\{-\left(\frac{1-\xi}{\xi}\right)\omega X_x \right. \\ &\quad \left. + \frac{1}{\xi}\left[\frac{1}{C_a} - \frac{1}{C_d}\left(\xi - 1 - \xi\frac{\sin\theta}{\theta}\right)\right]\right\}(-\sin\theta) \\ &\quad + \left[\left(\frac{1-\xi}{\xi}\right)\omega R_x - \frac{1-\cos\theta}{\theta C_d}\right](1-\cos\theta) \\ &= \omega\left(\frac{1-\xi}{\xi}\right)[R_x(1-\cos\theta) + X_x\sin\theta] \\ &\quad - \frac{\sin\theta}{\xi C_a} + \frac{1}{C_d}\left[\left(1 - \frac{1}{\xi} - \frac{\sin\theta}{\theta}\right)\right. \\ &\quad \left. \cdot \sin\theta - \frac{(1-\cos\theta)^2}{\theta}\right] \end{aligned} \tag{A.6}$$

$$\begin{aligned} &\text{Re}\,[DF^*] \\ &= \left[-\omega X_x + \frac{1}{C_d}\left(1 - \frac{\sin\theta}{\theta}\right)\right] \\ &\quad \cdot \left(\frac{1}{\xi} - 1 + \cos\theta\right) - \left[\omega R_x + \frac{1}{C_d}\cdot\left(\frac{1-\cos\theta}{\theta}\right)\right]\sin\theta \\ &= \omega\left[-R_x\sin\theta - X_x\left(\frac{1}{\xi} - 1 + \cos\theta\right)\right] \\ &\quad + \frac{1}{C_d}\left[\frac{1}{\xi}\left(1 - \frac{\sin\theta}{\theta}\right) - (1\cos\theta)\right] \end{aligned} \tag{A.7}$$

and

$$\begin{aligned} \text{Im}\,[DF^*] &= \left(\omega R_x + \frac{1-\cos\theta}{C_d\theta}\right)\left(\frac{1}{\xi} - 1 + \cos\theta\right) \\ &\quad + \left[-\omega X_x + \frac{1}{C_d}\left(1 - \frac{\sin\theta}{\theta}\right)\right]\sin\theta \\ &= \omega\left[R_x\left(\frac{1}{\xi} - 1 + \cos\theta\right) - X_x\sin\theta\right] \\ &\quad + \frac{1}{C_d}\left[\frac{1}{\xi}\left(\frac{1-\cos\theta}{\theta}\right)\right. \\ &\quad \left. + \sin\theta\left(1 - \frac{\sin\theta}{\theta}\right) - \frac{(1-\cos\theta)^2}{\theta}\right]. \end{aligned} \tag{A.8}$$

Therefore

$$\begin{aligned} \text{Re}\,[AB^* - DF^*] &= \frac{\omega}{\xi}(R_x\sin\theta + X_x\cos\theta) \\ &\quad + \frac{1-\cos\theta}{\xi C_a} - \frac{1}{\xi C_d}\left(\cos\theta - \frac{\sin\theta}{\theta}\right) \end{aligned} \tag{A.9}$$

and

$$\begin{aligned} \text{Im}\,[AB^* - DF^*] &= \frac{\omega}{\xi}(-R_x\cos\theta + X_x\sin\theta) \\ &\quad - \frac{\sin\theta}{\xi C_a} - \frac{1}{\xi C_d}\left(\sin\theta + \frac{1-\cos\theta}{\theta}\right). \end{aligned} \tag{A.10}$$

Note that

$$C_{-1}^{-1} = \bar{C}_1^{-1}e^{-j\phi} = \frac{1}{\bar{C}_1}(\cos\phi - j\sin\phi)$$

and

$$\begin{aligned} &2\,\text{Re}\,[C_{-1}^{-1}M_1(AB^* - DF^*)] \\ &= \frac{2M_1}{\bar{C}_1}[\text{Re}\,(AB^* - DF^*)\cos\phi \\ &\quad + \text{Im}\,(AB^* - DF^*)\sin\phi] \\ &= \frac{2M_1}{\bar{C}_1\xi}\left\{\cos\phi\left[(R_x\sin\theta + X_x\cos\theta)\omega\right.\right. \\ &\quad \left. + \frac{1-\cos\theta}{C_a} - \frac{1}{C_d}\left(\cos\theta - \frac{\sin\theta}{\theta}\right)\right] \\ &\quad + \sin\phi\left[(-R_x\cos\theta + X_x\sin\theta)\omega\right. \\ &\quad \left.\left. - \frac{\sin\theta}{C_a} - \frac{1}{C_d}\left(\sin\theta + \frac{1-\cos\theta}{\theta}\right)\right]\right\} \\ &= \frac{2\omega M_1}{\bar{C}_1\xi}[R_x\sin(\theta-\phi) \\ &\quad + X_x\cos(\theta-\phi) + f] \end{aligned} \tag{A.11}$$

where

$$\begin{aligned} f &= \frac{1}{\omega C_T}[\cos\phi - \cos(\theta-\phi)] \\ &\quad + \frac{1}{\omega C_D}\left[-\cos\phi - \left(\frac{1-\cos\theta}{\theta}\right)\sin\phi\right. \\ &\quad \left. + \frac{\sin\theta}{\theta}\cos\phi\right] \end{aligned}$$

and

$$\frac{1}{C_T}=\frac{1}{C_a}+\frac{1}{C_d}.$$

Appendix B

Here the first term of (15) is written in terms of the diode parameters and circuit impedance for $M_1 = M_{1T} = 1$. The subscript 0 is omitted for convenience

$$|A_0|^2(1-|S_0|^2)=|A|^2-|D|^2.$$

The $|A|^2$ can be expressed as

$$|A|^2=\left|j\omega\left(\frac{1-\xi}{\xi}\right)(Z_d+Z_x)\right|^2$$
$$=\omega^2\left(\frac{1-\xi}{\xi}\right)^2[(R_x+R_d)^2+(X_x+X_d)^2] \quad \text{(B.1)}$$

where

$$R_d=\frac{1}{\omega C_d}\left(\frac{\xi}{\xi-1}\cdot\frac{1-\cos\theta}{\theta}\right)$$

and

$$X_d=-\frac{1}{\omega C_a}\left(\frac{1}{1-\xi}\right)-\frac{1}{\omega C_d}\left(1-\frac{\xi}{\xi-1}\frac{\sin\theta}{\theta}\right).$$

The $|D|^2$ can be expressed as

$$|D|^2=\left|j\omega\left(Z_x+\frac{1-k}{j\omega C_d}\right)\right|^2$$
$$=\omega^2\left\{\left[R_x+\frac{1}{\omega C_d}\left(\frac{1-\cos\theta}{\theta}\right)\right]^2+\left[X_x-\frac{1}{\omega C_d}\left(1-\frac{\sin\theta}{\theta}\right)\right]^2\right\}. \quad \text{(B.2)}$$

Therefore

$$\frac{1}{\omega^2}(|A|^2-|D|^2)$$
$$=\left[\left(\frac{1-\xi}{\xi}\right)^2-1\right](R_x^2+X_x^2)$$
$$+2\left[\left(\frac{1-\xi}{\xi}\right)^2R_d-\frac{1}{\omega C_d}\cdot\left(\frac{1-\cos\theta}{\theta}\right)\right]\cdot R_x$$
$$+2\left[\left(\frac{1-\xi}{\xi}\right)^2X_d+\frac{1}{\omega C_d}\left(1-\frac{\sin\theta}{\theta}\right)\right]\cdot X_x$$
$$+\left(\frac{1-\xi}{\xi}\right)^2\cdot\left\{R_d^2+X_x^2-\left(\frac{1}{\omega C_d}\right)^2\cdot\left[\left(\frac{1-\cos\theta}{\theta}\right)^2+\left(1-\frac{\sin\theta}{\theta}\right)^2\right]\right\}$$
$$\triangleq\left[\left(\frac{1-\xi}{\xi}\right)^2-1\right]\cdot[(R_x-R_c)^2+(X_x-X_c)^2-r^2] \quad \text{(B.3)}$$

where

$$R_c=\left[\left(\frac{1-\xi}{\xi}\right)^2R_d-\frac{1}{\omega C_d}\left(\frac{1-\cos\theta}{\theta}\right)\right]\frac{\omega^2}{g}$$
$$=-\left(\frac{1-\cos\theta}{\omega\theta C_d}\frac{-1}{\xi}\right)\frac{\omega^2}{g}$$
$$X_c=-\left[\left(\frac{1-\xi}{\xi}\right)^2X_d+\frac{1}{\omega C_d}\left(1-\frac{\sin\theta}{\theta}\right)\right]\frac{\omega^2}{g}$$
$$=-\left\{\frac{\xi-1}{\xi^2}\frac{1}{\omega C_a}+\left[1-\left(\frac{1-\xi}{\xi}\right)^2-\frac{\sin\theta}{\xi\theta}\right]\frac{1}{\omega C_d}\right\}\frac{\omega^2}{g}$$
$$-r^2=\frac{\omega^2}{g}\left\{\left(\frac{1-\xi}{\xi}\right)^2[R_d^2+X_d^2]-\left(\frac{1}{\omega C_d}\right)^2\left[\left(\frac{1-\cos\theta}{\theta}\right)^2+\left(1-\frac{\sin\theta}{\theta}\right)^2\right]\right\}-(X_c^2+R_c^2)$$

and

$$g=\omega^2\left[\left(\frac{1-\xi}{\xi}\right)^2-1\right].$$

Thus $|A|^2-|D|^2=0$ is a circle in the complex impedance plane with radius r and center at (R_c,X_c). Identical results were obtained in [3].

Acknowledgment

The authors wish to thank Mr. P. Bauhahn for valuable discussions.

References

[1] M. E. Hines, "Large signal noise, frequency conversion and parametric instabilities in IMPATT diode networks," *Proc. IEEE*, vol. 60, pp. 1534–1548, Dec. 1972.

[2] D. F. Peterson, "Circuit conditions to prevent second-subharmonic power extraction in periodically driven IMPATT diode networks," *IEEE Trans. Microwave Theory Tech.*, vol. MTT-22, pp. 784–790, Aug. 1974.

[3] W. E. Schroeder, "Spurious parametric oscillations in IMPATT circuits," *Bell Syst. Tech. J.*, vol. 53, no. 7, pp. 1187–1210, Sept. 1974.

[4] P. A. Blakey, B. Culshaw, and R. A. Giblin, "Efficiency enhancement in avalanche diodes by depletion-region-width modulation," *Electron. Lett.*, vol. 10, no. 21, pp. 435–438, Oct. 17, 1974.

[5] R. L. Kuvås and W. E. Schroeder, "Premature collection mode in IMPATT diodes," in *Int. Electron Devices Meeting Tech. Digest*, Washington, D.C., Dec. 1974, pp. 134–137.